ON THE ORIGIN OF THE HELIOSPHERIC MAGNETIC FIELD POLARITY INVERSION AT HIGH LATITUDES

S. Landi[(1)], P. Hellinger[(1,2)], and M. Velli[(1,3)]

[(1)] *Department of Astronomy and Space Science, Univ. of Firenze, 50125 Firenze, Italy*
[(2)] *Institute of Atmospheric Physics, Prague, Czech Republic*
[(3)] *Jet Propulsion Laboratory, California Instiute of Technology, Pasadena 91109, CA*

ABSTRACT

High latitude observations of the magnetic field by the Ulysses spacecraft have shown a significant number of cases where the radial magnetic field polarity is reversed with respect to the dominant polarity of the coronal hole from which the wind emanates. Such reversals have the nature of folded back magnetic field lines. It has been suggested that such reversals are due to reconnection of closed and open field lines in the lower corona which would launch a large amplitude Alfvén wave into the solar wind. The kink in the field line however is unstable and disappears within a few dynamical time-scales. We suggest an alternative mechanism for the generation of the polarity reversal, namely, the coupling of standard large amplitude Alfvén turbulence in the low frequency regime propagating away from the sun with the micro-stream shears observed in the high speed solar wind. In this way reversals are generated naturally during propagation from the sun in a time-scale consistent with their observation by Ulysses.

1. INTRODUCTION

White light and EUV observations show the solar corona to be finely structured even in coronal holes, with rays and plumes persisting out to the largest distances observable using coronagraphs in space, about 30Rs (LASCO). On the other hand, extensive studies by the Ulysses mission in situ have shown that many different plasma and magnetic field structures, which span a large interval of time scales - from several hours to days -, are present in the out-of-ecliptic fast solar wind, presumably originating from coronal holes: pressure balance structures (McComas et al. 1995, 1996), micro-streams (McComas et al. 1995; Neugebauer et al. 1995), magnetic holes, radial magnetic field polarity inversions (Balogh et al. 1999), as well as the ever present large scale Alfvén wave spectrum (Smith et al. 1995) propagating away from the sun. Though there have been attempts to identify the connection or at least correlate structures measured in-situ with the fine structure of coronal holes observed closer to the sun, there is no unequivocally determined coronal remnant recognized in the fast wind, the difficulty being probably due to the strong dynamical evolution occurring from the solar wind acceleration region outwards.

The fast solar wind carries magnetic field lines with a polarity which corresponds on average to the dominant polarity in the photosphere from which the wind originates (Balogh et al. 1995; Forsyth et al. 1996b). However, high-latitude observations show a statistically significant number of cases where the magnetic field polarity is inverted (Balogh et al. 1999). Earlier studies from Balogh et al. (1999) have shown that, during these inversions, the velocity-magnetic field correlation in the Alfvénic turbulence spectrum corresponds to Alfvén waves that propagate sunward, an indication that the measurement of a radial magnetic field inversion corresponds to a passage across a fold in a unipolar field, rather than a period of opposite polarity flux connecting all the way back to the sun. Yamauchi et al. (2002), based on the minimum variance analysis, conclude that polarity inversions observed within pressure balance structures have the character of tangential discontinuities, differing from those observed outside pressure balance structures where they have the character of rotational discontinuities. However, the analysis of the differential velocity between protons and alpha particles indicate that these two types of polarity inversions are similar (Yamauchi et al. 2004b): both are likely switch-backs of magnetic field lines (cf. Yamauchi et al. 2004b, Figure 1) . These results led Yamauchi et al. (2004a) to suggest that the observed magnetic field polarity inversion could be produced at the sun by the eruption of macrospicule-size magnetic loops from the magnetic network. The erupting magnetic field loop could then become a magnetic field switchback in the fast solar wind if reconnection with the open magnetic field line of the polar hole is not fully completed after the loop enters in the solar wind acceleration region.

We use here a 2.5D magnetohydrodynamic (MHD) numerical model to test the above suggestion as well as outline an alternative scenario for the formation of such structures. We have followed the evolution of a large amplitude Alfvén wave containing a well defined region with reverse polarity in the magnetic field. The simulations show that this structure, as expected on dimensional grounds, does not survive beyond distances of a few tens of thousands of kilometers. Using the same numerical model we have studied the interaction between a sheared velocity structure, modeling the fast wind micro-streams, and a magnetic field containing a component across the shear, such as arising from the lowest frequency range of outwardly propagating Alfvénic turbulence. The simulations show that switch-backs are produced. In the region where the inversion of the magnetic field occurs there is an enhancement of the gas pressure and a drop in the magnetic field pressure. The total pressure remains approximatively constant and the plasma β grows with respect to the adjacent regions. The simulation therefore suggests that magnetic field polarity inversions could be produced in situ by the interaction of low frequency, high

Proc. Solar Wind 11 – SOHO 16 "Connecting Sun and Heliosphere", Whistler, Canada
12 – 17 June 2005 (ESA SP-592, September 2005)

amplitude, transverse Alfvén waves with radial velocity field fluctuations.

2. THE NUMERICAL MODEL

We make use of the visco-resistive MHD equations for an isothermal plasma

$$\frac{\partial \rho}{\partial t} + \nabla \cdot (\rho \mathbf{v}) = 0 \quad (1)$$

$$\frac{\partial \mathbf{v}}{\partial t} + \mathbf{v} \cdot \nabla \mathbf{v} = -\frac{c^2}{\rho} \nabla \rho + (\nabla \times \mathbf{B}) \times \mathbf{B} + \frac{1}{R_\nu} \nabla^2 \mathbf{v} \quad (2)$$

$$\frac{\partial \mathbf{B}}{\partial t} = \nabla \times (\mathbf{v} \times \mathbf{B}) + \frac{1}{R_\eta} \nabla^2 \mathbf{B} \quad (3)$$

Here $\mathbf{v}$ is the fluid velocity, $\mathbf{B}$ the magnetic field and ρ the density. $c^2 = R/\mu T$, with R the gas constant and $\mu = 1/2$ the mean atomic weight for a fully ionized plasma of electrons and protons, is the isothermal sound speed. These equations are expressed in dimensionless units, defining a characteristic length L_0, a characteristic density ρ_0 and a characteristic magnetic field strength B_0. The velocity field as well the isothermal sound speed are therefore expressed in units of the Alfvén speed $v_a = \sqrt{B^2/(4\pi\rho)}$ while the characteristic time scale is the Alfvén crossing time $t_a = L_0/v_a$. The magnitude of the dissipative terms are determined by the magnetic $R_\eta = L_0 v_a/\eta_0$ and the kinetic $R_\nu = L_0 v_a/\nu_0$ Reynolds numbers. We assume an ignorable coordinate, z, and introduce a scalar potential function ϕ so that

$$\mathbf{B} = \left(\frac{\partial \phi}{\partial y} + B_{x0}\right) \hat{x} - \left(\frac{\partial \phi}{\partial x} - B_{y0}\right) \hat{y} + B_z \hat{z} \quad (4)$$

with B_{x0} and $B_y 0$ constants. The equations (1),(2) and (3) are integrated in a rectangular box of dimensions $[-L_x, L_x] \times [-L_y, L_y]$ and the boundary conditions are assigned by the use of projected characteristics of the MHD equations (Vanajakshi et al. 1989; Roe & Balsara 1996), allowing us to have essentially perfect non-reflecting boundary conditions. Spatial integration is performed by the use of compact difference schemes (Lele 1992) while time integration is performed with a third order Runge-Kutta method.

3. KINK ALFVÉN WAVES

The basic idea for a solar origin of the magnetic field switch-backs observed in the high latitude fast solar wind is magnetic loop eruptions an subsequent reconnection with an open field line allowing a kink to propagate outward (Yamauchi et al. 2004a, Fig. 1). The kink Alfvén wave can be represented by the function ϕ using the following profile

$$\phi = -\phi_0 \left(\mathrm{e}^{-r_1^2} - \mathrm{e}^{-r_2^2}\right) \quad (5)$$

with

$$r_{1,2}^2 = \left((x - x_{1,2})/\lambda_x\right)^2 + \left((y - y_{1,2})/\lambda_y\right)^2 \quad (6)$$

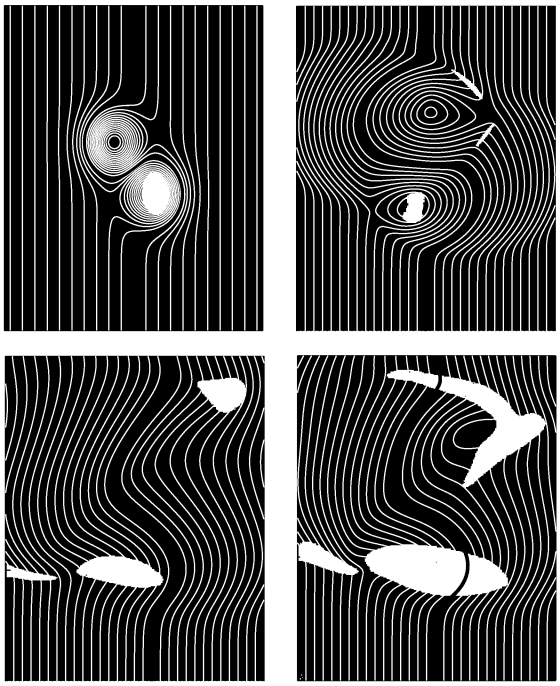

Figure 1. Temporal evolution of the magnetic field line (white) and current density grey-scale for a magnetic field inversion created by a large amplitude kink Alfvén wave containing a magnetic field switchback. Central magnetic field line is emphasized in black. Clockwise from top left t=0 s, 50 s, 100 s, 150 s

The width $\lambda_{x,y}$ as well as the values $(x_{1,2}, y_{1,2})$ are chosen in order to have a well defined magnetic inversion polarity in the middle of the simulation domain

$$\begin{array}{lll} y_1 = 1 & y_2 = -1 & \lambda_y = 1 \\ x_1 = 1.5 & x_2 = -0.5 & \lambda_x = 1/\sqrt{3} \end{array} \quad (7)$$

The wave propagates along a constant magnetic field $B_0 = B_0 \hat{y}$ in the vertical y direction, and its Alfvénicity is characterized by an anticorrelated velocity field $\delta \mathbf{v} = -\delta \mathbf{b}/\sqrt{\rho}$ The simulation rest frame is moving at the constant Alfvén velocity due to the field B_0 . The initial condition magnetic field lines are shown in the upper left panel of Fig. 1.

For a typical density $n_0 = 10^8$ cm^{-3} and a typical magnetic field strength $B_0 = 10$ G the Alfvén velocity is $v_a = 2000$ km/s. Macrospicule magnetic loops are supposed to have dimensions of order $L_0 = 10000$ Km(Yamauchi et al. 2004a). Therefore the characteristic time scale t_a is around 5 s. For a 10^6K corona the sound speed is approximatively equal to $c = 130$ km/s and the plasma β is approximatively $8 \cdot 10^{-3}$.

Fig. 1 shows the evolution of the magnetic field lines as function of time. The kink wave is not in pressure equilibrium with the surrounding magnetic field and as a consequence expands. During the expansion the unperturbed field lines are compressed and distorted. The Alfvén wave also has vorticity and tends to turn clockwise or anti-clockwise, in order to reduce the magnetic

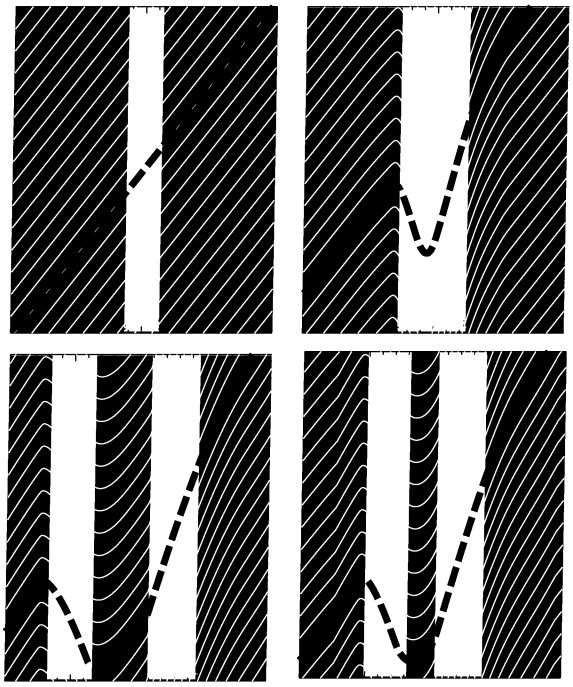

Figure 2. Temporal evolution of the magnetic field line and velocity field intensity for a simulation where an initial magnetic field (white lines, central one in black dash) is stretched by an unaligned velocity shear, whose intensity is shown in grey-scale. The velocity field is directed in the vertical direction and vanishes in the center - i.e. the bright regions are regions of lower velocity. Times are shown clockwise from upper left 0 h, 2 h, 4 h, 6h.

stress. The result is that the structure is rapidly destroyed. After 20 $\mathrm{t_a}$ the magnetic field has recovered the dominant polarity of the unperturbed magnetic field. Therefore the inversion of the magnetic field lines lasts only over a length $d = 20 v_a t_a = 20 L_0 \sim 2 \cdot 10^5$ Km. With the typical Reynolds number and resolutions used here the dissipative time scales are much higher than the dynamical time scales, so the evolution is driven by the ideal tendency of the field line to unbend.

4. SHEAR

In this simulation we model the low-frequency part of Alfvnic turbulence - which is dominated by the magnetic fluctuations - with a perturbed transverse magnetic field, which for simplicity is assumed constant on the scale of the numerical domain. This fluctuation is embedded in a velocity stream. The magnetic field initially forms an angle θ with the shear. In the simulations the velocity field is directed along the y-direction and has the following profile:

$$\mathbf{u} = -\delta u_0 \exp -\frac{(x-\pi)^2}{2\delta^2} \hat{y} \tag{8}$$

where δ is the half width of the stream and δu_0 its amplitude. The magnetic field is taken initially to be

$$\mathbf{B} = b_0 \left(\cos\theta \hat{x} + \sin\theta \hat{y}\right) = b_{x0}\hat{x} + b_{y0}\hat{y} \tag{9}$$

Typical Alfvén speeds in the fast solar wind are few tens of kilometers per second while Ulysses observations have shown that fluctuations of the velocity field are of the order of 50 $\mathrm{km/s}$ (McComas et al. 1995; Neugebauer et al. 1995). So for the simulations we choose $b_0 = 1$ and δu between 2 and 5. The plasma β in fast solar wind streams varies between 2 and 5 (McComas et al. 1995, 1996) and can reach values of 10, 20 in the PBSs(Yamauchi et al. 2004b). The mean angle between the magnetic field line and the flow can span a large interval: during the Ulysses orbit the Parker's spiral azimuth angle varies between 80° near the ecliptic at 5.4 AU to 40° at latitude 60° and 3.2 AU (Forsyth et al. 1996b,a). Magnetic field fluctuations are present as long period and large amplitude Alfvén waves also at helio-latitudes greater than 60° (Forsyth et al. 1996b; Smith et al. 1995; Neugebauer 2004). For our simulations we have chosen an angle of 45°as a representative value. If the characteristic period of the Alfvn wave is an hour, a local Alfvén velocity of 20 $\mathrm{Km/s}$ (Smith et al. 1995; Goldstein et al. 1995) implies that the typical length scale of our simulations is $L_0 = 72000$ Km corresponding to the width of the velocity shear δ.
In Fig. 2 the magnetic field lines and the intensity of the velocity shear are shown for different times. The plasma β has been taken equal to 5 while the ratio between the minimum velocity of the shear and the Alfvén velocity has been chosen equal to 5, not far from what is seen in high speed streams. The flow drags the magnetic field lines distorting them and a switchback develops. The time scale for this to occur can be found on dimensional grounds, since the growth is driven by the stream gradient, and it is the transverse field which must be bent back into a field whose magnitude is of the same order of the initial radial field:

$$\delta t = \frac{b_{y0}}{b_{x0}} \frac{2\delta}{\delta u}. \tag{10}$$

With the values of the simulations shown in Fig. 2 we obtain $\delta t = 0.4$ in very good agreement with the time when the inversion occur in the simulation. In Fig. 3 the profiles of the stream-wise component of the magnetic field as a function of the cross-stream direction y are shown at $t = 2$. The magnetic field reverses its polarity between $y = 3\pi/4$ and $y = 7\pi/8$. In correspondence with the polarity inversion there is a drop in the magnetic pressure (dotted line in the third panel of Fig. 3) and an increase in the plasma pressure (dashed line of the same panel). The total pressure remains almost constant (solid line) and the plasma β increases of roughly a factor 5 with respect to the adjacent regions.

5. CONCLUSION

In the solar corona the magnetic pressure largely exceeds the plasma pressure. A magnetic field topology which

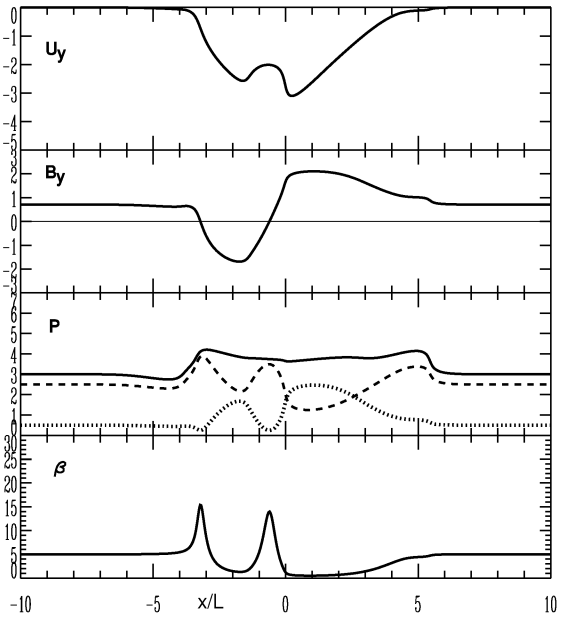

Figure 3. From top to bottom, cross-stream profiles of the velocity shear, x-component of the magnetic field, total (solid), thermal (dashed) and magnetic (dotted) pressures, and plasma β for the simulation of Fig. 2 at time $t = 2$

contains switchback field lines is hardly confined by the surrounding plasma pressure. The magnetic stress of this topology is free to expand on time scales comparable to the local characteristic Alfvén time and the polarity inversion is suppressed over scale heights of few tens of thousands kilometers. While the simulations shown here do not mean to exclude that this mechanism can occur in the solar corona, they indicate that switch-backs in the magnetic field lines formed in the corona should not survive up to distances where they are observed by the Ulysses spacecraft.

Although in the fast polar solar wind the mean magnetic field is essentially radial, several transient futures cause the magnetic field to be unaligned with respect to the flow direction. Magnetic field fluctuations are observed over a broad frequency range, corresponding to a well-developed spectrum of outwardly propagating Alfvén waves in a well-defined interval. At frequencies below 10^{-5} Hz fluctuations generated in the corona and advected out in the solar wind lose their Alfvénic correlation rapidly, and magnetic field fluctuations in this regime decay more slowly with distance from the sun, leading to an increase in deviations of the magnetic field from the radial with distance from the sun ((Jokipii & Kota 1989)). Some evidence of the existence of such very low frequency fluctuations has been reported by Jokipii et al. (1995) and Smith et al. (1997). In any case, in the low frequency range (below 10^{-4} Hz) the observed amplitudes of magnetic field fluctuations are of the same order of the mean magnetic field $\delta b/b \sim 1$. Such magnetic field fluctuations can interact quickly with a velocity shear fluctuation, such as that determined by micro-streams ((McComas et al. 1995; Neugebauer et al. 1995)), given the fact that the plasma pressure exceeds the magnetic field pressure and the fluctuations in the velocity field are greater than the local Alfvén speed. The magnetic field lines are then dragged by the velocity shear and they are distorted until the polarity changes sign. Our numerical simulations show how this interaction leads not only to the radial field inversions, but also to plasma pressure and density signals similar to those observed in the data.

ACKNOWLEDGMENTS

This work has been partially supported by the Research Training Network (RTN) Theory, Observation, and Simulation of Turbulence in Space Plasmas, funded by the European Commission (contract HPRN-CT-2001-00310). MV acknowledges the support of NASA.

REFERENCES

Balogh, A., Forsyth, R. J., Lucek, E. A., Horbury, T. S., & Smith, E. J. 1999, Geophys. Res. Lett., 26, 631

Balogh, A., Smith, E. J., Tsurutani, B. T., et al. 1995, Science, 268, 1007

Forsyth, R. J., Balogh, A., Horbury, T. S., et al. 1996a, Astron. Astrophys., 316, 287

Forsyth, R. J., Balogh, A., Smith, E. J., Erdös, G., & McComas, D. J. 1996b, J. Geophys. Res., 101, 395

Goldstein, B. E., Neugebauer, M., & Smith, E. J. 1995, Geophys. Res. Lett., 22, 3389

Jokipii, J. R., Kóta, J., Giacalone, J., Horbury, T. S., & Smith, E. J. 1995, Geophys. Res. Lett., 22, 3385

Jokipii, J. R. & Kota, J. 1989, Geophys. Res. Lett., 16, 1

Lele, S. K. 1992, J. Comp. Phys., 103, 16

McComas, D. J., Barraclough, B. L., Gosling, J. T., et al. 1995, J. Geophys. Res., 100, 19893

McComas, D. J., Hoogeveen, G. W., Gosling, J. T., et al. 1996, Astron. Astrophys., 316, 368

Neugebauer, M. 2004, J. Geophys. Res., 109, A02101

Neugebauer, M., Goldstein, B. E., McComas, D. J., Suess, S. T., & Balogh, A. 1995, J. Geophys. Res., 100, 23389

Roe, P. L. & Balsara, D. S. 1996, J. Appl. Math., 56, 57

Smith, E. J., Balogh, A., Neugebauer, M., & McComas, D. 1995, Geophys. Res. Lett., 22, 3381

Smith, E. J., Neugebauer, M., Tsurutani, B. T., et al. 1997, Adv. Space Res., 20, 55

Vanajakshi, T. C., Thompson, K. W., & Black, D. C. 1989, J. Comp. Phys., 84, 343

Yamauchi, Y., Moore, R. L., Suess, S. T., Wang, H., & Sakurai, T. 2004a, Astrophys. J., 605, 511

Yamauchi, Y., Suess, S. T., & Sakurai, T. 2002, Geophys. Res. Lett., 29, 21

Yamauchi, Y., Suess, S. T., Steinberg, J. T., & Sakurai, T. 2004b, J. Geophys. Res., 109, A03104